

# The Human Novel Gene *LNC-HC* Inhibits Hepatocellular Carcinoma Cell Proliferation by Sequestering *hsa-miR-183-5p*

Xi Lan,<sup>1,2</sup> Nan Wu,<sup>1,2</sup> Litao Wu,<sup>1,2</sup> Kai Qu,<sup>3</sup> Ezra Kombo Osoro,<sup>1,2</sup> Dongxian Guan,<sup>4</sup> Xiaojuan Du,<sup>1,2</sup> Bo Wang,<sup>5</sup> Sifan Chen,<sup>6</sup> Ji Miao,<sup>4</sup> Juan Ren,<sup>7</sup> Li Liu,<sup>8</sup> Haiyun Li,<sup>1,2</sup> Qilan Ning,<sup>1,2</sup> Dongmin Li,<sup>1,2</sup> and Shemin Lu<sup>1,2</sup>

<sup>1</sup>Department of Biochemistry and Molecular Biology, School of Basic Medical Sciences, Xi'an Jiaotong University Health Science Center, Xi'an, Shaanxi 710061, China; <sup>2</sup>Key Laboratory of the Environment and Genes Related to Diseases, Xi'an Jiaotong University, Ministry of Education of China, Beijing, China; <sup>3</sup>Department of Hepatobiliary Surgery, The First Affiliated Hospital of Xi'an Jiaotong University, Xi'an, Shaanxi 710061, China; <sup>4</sup>Division of Endocrinology, Boston Children's Hospital, Harvard Medical School, Boston, MA, USA; <sup>5</sup>Center for Translational Medicine, The First Affiliated Hospital of Xi'an Jiaotong University, Shaanxi 710061, China; <sup>6</sup>Medical Research Center, Sun Yat-Sen Memorial Hospital, Sun Yat-Sen University, Guangzhou, China; <sup>7</sup>Department of Reproductive Medicine, The Fourth Hospital of Xi'an, Xi'an, Shaanxi 710004, China; <sup>8</sup>Department of Basic Medical Science, Xi'an Medical College, Xi'an, Shaanxi, China

**Hepatocellular carcinoma (HCC) is the most commonly diagnosed cancer and the leading cause of cancer mortality. Several lines of evidence have demonstrated the aberrant expression of long noncoding RNAs (lncRNAs) in carcinogenesis and their universal regulatory properties. A thorough understanding of lncRNA regulatory roles in HCC pathology would contribute to HCC prevention and treatment. In this study, we identified a novel human lncRNA, *LNC-HC*, with significantly reduced levels in hepatic tumors from patients with HCC. MTT (3-(4,5-dimethylthiazol-2-yl)-2,5-dimethyltetrazolium bromide) assays as well as colony formation and wound healing experiments showed that *LNC-HC* significantly inhibited the proliferation of the HCC cell line Huh7. Xenograft transplantation of *LNC-HC*-overexpressing Huh7 cells in nude mice resulted in the production of smaller tumors. Mechanistically, *LNC-HC* inhibited the proliferation of HCC cells by directly interacting with *hsa-miR-183-5p*. *LNC-HC* rescued the expression of five tumor suppressors, including *AKAP12*, *DYRK2*, *FOXN3*, *FOXO1*, and *LATS2*, that were verified as target genes of *hsa-miR-183-5p*. Overall, human *LNC-HC* was identified as a novel tumor suppressor that could inhibit HCC cell proliferation *in vitro* and suppress tumor growth *in vivo* by competitively binding *hsa-miR-183-5p* as a competing endogenous RNA (ceRNA). These findings suggest that *LNC-HC* could be a biomarker of HCC and provide a novel therapeutic target for HCC treatment.**

Long noncoding RNAs (lncRNAs) are a type of RNAs that are longer than 200 nt and traditionally defined as not having translation potential; however, recent studies have shown that some lncRNAs could produce short functional peptides.<sup>4,5</sup> An increasing number of studies have verified that lncRNAs play a large role in biological processes. Some lncRNAs function as coregulators of proteins that directly combine with coregulator proteins to regulate downstream tumor-related gene expression.<sup>6-12</sup> Furthermore, another class of lncRNAs functions as competing endogenous RNAs (ceRNAs).<sup>13-15</sup> This class of lncRNAs sequesters microRNAs by acting as a sponge and controls the expression of microRNA-targeted oncogenes or tumor repressors. A well-studied lncRNA, lncRNA-ATB, induces epithelial-mesenchymal transition (EMT) and the invasion of cancer cells through up-regulating ZEB1 and ZEB2 expression by acting as a ceRNA for miR-200.<sup>13</sup> In addition, the tumorigenic lncRNA HULC also functions as a ceRNA through sequestering miR-372, resulting in the upregulation of an oncogene in liver cancer.<sup>14</sup> These findings revealed that the aberrant expression of lncRNAs plays a role in cell proliferation, angiogenesis, and tumor development. The identification of novel lncRNAs and the exploration of their functions and regulatory molecular mechanisms could provide promising therapeutic targets for liver cancer.

In our previous study, a novel rat lncRNA, *lnc-HC*, was identified in rat hepatocytes as a regulator of hepatocyte cholesterol

## INTRODUCTION

Hepatocellular carcinoma (HCC) is a commonly diagnosed malignancy and the leading cause of cancer death worldwide and it has shown an increasing incidence compared to that of other cancers.<sup>1-3</sup> Although improvements have been made in surgical and therapeutic techniques, the 5-year survival rate of HCC patients is still unsatisfactory. The molecular mechanisms underlying liver cancer pathology need to be further explored.

Received 7 February 2020; accepted 17 March 2020;  
<https://doi.org/10.1016/j.omtn.2020.03.008>

**Correspondence:** Xi Lan, Department of Biochemistry and Molecular Biology, School of Basic Medical Sciences, Xi'an Jiaotong University Health Science Center, Xi'an, Shaanxi 710061, China.

**E-mail:** [lanxi.2016@xjtu.edu.cn](mailto:lanxi.2016@xjtu.edu.cn)

**Correspondence:** Shemin Lu, Department of Biochemistry and Molecular Biology, School of Basic Medical Sciences, Xi'an Jiaotong University Health Science Center, Xi'an, Shaanxi 710061, China.

**E-mail:** [lushemin@xjtu.edu.cn](mailto:lushemin@xjtu.edu.cn)





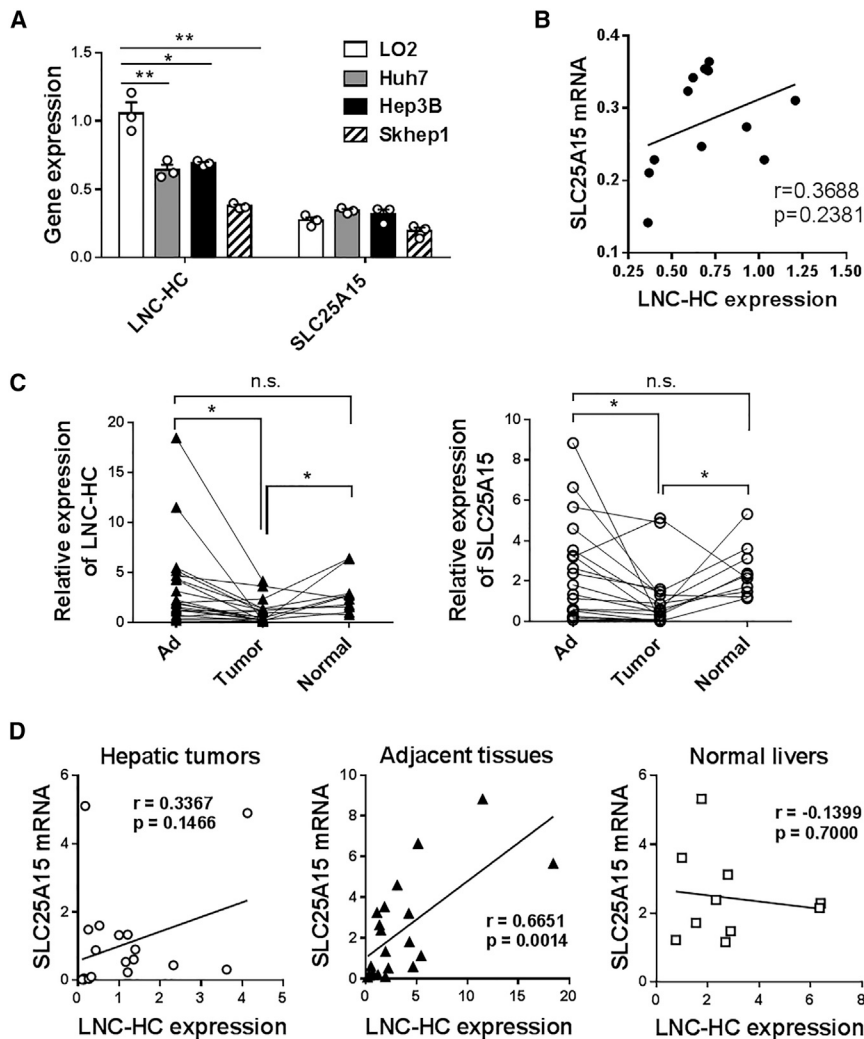


**Figure 2. *LNC-HC* Expression Was Significantly Reduced in Both HCC Cell Lines and Clinical Hepatic Tumor Tissues**

(A) Quantitative real-time PCR detection of *LNC-HC* and *SLC25A15* mRNA levels in the human hepatocyte cell line LO2 and the HCC cell lines Huh7, Hep3B, and Skhep1. (B) Correlation analysis of *LNC-HC* and *SLC25A15* expression in four types of cell lines at the mRNA level. (C) Quantitative real-time PCR detection of *LNC-HC* and *SLC25A15* expression in 20 hepatic tumor tissues, 20 paired adjacent non-tumor tissues, and 10 paired normal tissues from HCC patients. (D) Correlation analysis of *LNC-HC* and *SLC25A15* expression in clinical liver samples at the mRNA level. Ad, adjacent non-tumor tissues. *ACTB* was used for normalization in the quantitative real-time PCR assay. \* $p < 0.05$ , \*\* $p < 0.01$ . n.s., not significant. Values are expressed as the means  $\pm$  SEM.

tissues; *SLC25A15* showed a similar expression pattern (Figure 2C). To check the correlation of the expression between *LNC-HC* and *SLC25A15* in clinical samples, a detailed analysis was performed. The two genes expressions were significantly correlated in adjacent tissues; however, no correlation was observed in tumor tissues and normal ones (Figure 2D). According to the median ratio of *LNC-HC* expression, HCC patients were divided into *LNC-HC*<sup>low</sup> and *LNC-HC*<sup>high</sup> groups. Clinicopathological analysis suggested that *LNC-HC* expression was more likely correlated with tumor size ( $p = 0.1409$ ) and tumor-node-metastasis (TNM) stage ( $p = 0.075$ ) as compared with other parameters, including age, sex, metastasis, carcinoembryonic antigen (CEA), and alpha-fetoprotein

(AFP) levels (Table 1). These findings suggest that *LNC-HC* might be a potential tumor suppressor in HCC.

#### ***LNC-HC* Inhibits Cell Proliferation *In Vitro***

To test the biological effects of *LNC-HC* on cell growth, *LNC-HC* and *SLC25A15* were overexpressed in Huh7 and LO2 cells to generate over*LNC-HC* Huh7/LO2 and over*SLC25A15* Huh7/LO2 cells, respectively (Figures 3A and 3B). An MTT (3-(4,5-dimethylthiazol-2-yl)-2,5-dimethyltetrazolium bromide) assay showed that *LNC-HC* overexpression significantly inhibited the proliferation of Huh7 cells *in vitro* compared with overexpressed negative control (NC) cells; *SLC25A15* overexpression had no effect (Figure 3C). Moreover, the overexpression of *LNC-HC* and *SLC25A15* did not affect the growth of LO2 cells within 72 h (Figure 3D). Consistently, *LNC-HC* overexpression suppressed Huh7 and LO2 cell colony formation (Figures 3E and 3F). A wound healing study showed that *LNC-HC* inhibited the migration of Huh7 and LO2 cells (Figure 3G). These results indicated that *LNC-HC* suppresses Huh7 cell growth *in vitro*.

Immunoblotting results showed that FLAG-tag protein was hardly detected in the *LNC-HC* group (Figure 1E, lower panel). EGFP-fusion protein showed the similar results (Figure 1F). Based on bioinformatics analysis and protein expression experiments, we confirmed that *LNC-HC* is a lncRNA and is the human homolog of the previously identified rat *lnc-HC*.

#### ***LNC-HC* Is Decreased in Hepatic Tumors in HCC**

Quantitative real-time PCR results showed that *LNC-HC* was significantly decreased in three types of HCC cell lines, including Huh7, Hep3B and Skhep1, compared with the human hepatocyte cell line LO2; *SLC25A15* showed no differences among these groups of cells (Figure 2A). In addition, there was no significant correlation between *LNC-HC* and *SLC25A15* expression in these four cell lines (Figure 2B). Among the 20 hepatic tumor tissues, the paired 20 adjacent non-tumor tissues and 10 normal liver tissues from 20 patients with HCC, *LNC-HC* was significantly decreased in the tumor tissues compared with the adjacent and normal liver

**Table 1. The Association between LNC-HC Expression and Clinicopathological Characteristics of the 20 HCC Patients**

Variable	All Patients (n)	LNC-HC Expression		p Value
		Low	High	
All cases	20	10	10	
<b>Age (years)</b>				
	15	8	7	>0.9999
≥60	5	2	3	
<b>Sex</b>				
Male	16	8	8	>0.9999
Female	4	2	2	
<b>Tumor size (cm)</b>				
	6	1	5	0.1409
≥5	14	9	5	
<b>TNM stage</b>				
I	2	1	1	0.075
II	4	0	4	
III	12	7	5	
IV	2	2	0	
<b>Lymphatic metastasis</b>				
Yes	2	1	1	>0.9999
No	18	9	9	
<b>Distant metastasis</b>				
Yes	2	1	1	>0.9999
No	18	9	9	
<b>CEA (ng/mL)</b>				
	13	5	8	0.3498
≥5	7	5	2	
<b>AFP (ng/mL)</b>				
	10	4	6	0.6563
≥400	10	6	4	

TNM, tumor-node-metastasis; CEA, carcinoembryonic antigen; AFP, alpha-fetoprotein.

### LNC-HC Inhibits Tumor Growth in a Mouse Xenograft Model

To check the effect of LNC-HC on tumor growth *in vivo*, we generated a xenograft tumor model by subcutaneously injecting <sup>overNC</sup>Huh7 and <sup>overLNC-HC</sup>Huh7 cells into BALB/c nude mice. Compared with <sup>overNC</sup>Huh7 cells, <sup>overLNC-HC</sup>Huh7 cells grew more slowly, as indicated by their smaller tumor volumes (Figures 4A–4C) and tumor weights (Figure 4D). These results showed that LNC-HC significantly suppresses tumor growth *in vivo*.

### LNC-HC Interacts with hsa-miR-183-5p

To determine the regulatory mechanism involved in the effects of LNC-HC on the antitumor process, we first examined the possibility of a ceRNA-like pattern. In the prediction of the interaction between mi-

croRNAs and LNC-HC by the miRDB software (<http://mirdb.org/>), six microRNA candidates with higher scores were obtained, including *hsa-miR-183-5p*, -4482, -10527, -4276, -5001, and -146a. Quantitative real-time PCR results suggested that *hsa-miR-183-5p* (hereafter referred to as *miR-183*) was significantly increased in tumor tissues compared with adjacent and normal tissues, while *miR-4482* and *miR-10527* expression were decreased in tumors compared with adjacent tissues (Figure 5A). Among the six candidates, *miR-183* expression in tumor tissues indicated that it might interact with LNC-HC to form a ceRNA regulatory system. *In vitro* experiments showed that the *miR-183* mimic significantly decreased LNC-HC expression both in Huh7 and LO2 cells (Figures 5B and 5C), whereas LNC-HC had no effect on *miR-183* expression (Figures S2A and S2B). In addition, the *miR-183* mimic facilitated Huh7 and LO2 cell proliferation; *miR-183* inhibited the suppression by LNC-HC of the proliferation of Huh7 cells (Figure 5D). To verify the direct interaction between *miR-183* and LNC-HC, we constructed dual-luciferase reporter gene vectors that contained wild-type and mutant *miR-183*-targeted LNC-HC sequences (1 and 2) using pmirGLO as a basic plasmid, which are referred to as pLNC-HC1-wt/mut and pLNC-HC2-wt/mut, respectively (Figure 5E). After the transfection of pLNC-HC1/2-wt/mut and the *miR-183* mimic, we found that *miR-183* decreased the luciferase activity of pLNC-HC1-wt and pLNC-HC2-wt but had no effect on the mutant plasmids in both Huh7 and LO2 cells (Figures 5F and 5G). These findings suggested that *miR-183* directly targets LNC-HC through binding regions 1 and 2; the two genes, a lncRNA and a microRNA, may form a ceRNA system to coregulate downstream gene expression.

### LNC-HC/miR-183 Coregulate the Expression of Tumor Repressors as ceRNA

To verify the ceRNA function of LNC-HC and *miR-183*, we predicted 16 tumor repressors that were directly targeted by *miR-183* using miRDB software. Among these candidates, 6 genes (*AKAP12*,<sup>18–20</sup> *FOXO1*,<sup>21–34</sup> *IDH2*,<sup>35–37</sup> *PDCD4*,<sup>38–46</sup> *PTEN*,<sup>47,48</sup> and *SOCS6*<sup>35,49</sup>) have previously been reported as *miR-183* targets; the other 10 genes (*ARHGDI1*, *CRKL*, *DDIT4*, *DYRK2*, *FOXN3*, *LATS2*, *PTPN12*, *RHOB*, *SMG-1*, and *SPRED1*) were the predicted candidates with the highest scores without experimental verification. In Huh7 cells, four of the verified genes (including *AKAP12*, *FOXO1*, *IDH2*, and *PDCD4*) and six of the predicted genes (including *CRKL*, *DDIT4*, *FOXN3*, *LATS2*, *PTPN12*, and *SMG-1*) were significantly suppressed by *miR-183* (Figures 6A and 6B). In LO2 cells, five of the verified genes (including *AKAP12*, *FOXO1*, *IDH2*, *PDCD4*, and *SOCS6*) and four of the predicted genes (including *DDIT4*, *DYRK2*, *LATS2*, and *SPRED1*) were suppressed by *miR-183* (Figures S3A and S3B). Next, we examined the effect of LNC-HC on the expression of these candidate genes. In Huh7 cells, LNC-HC overexpression increased the expression of four genes both at the mRNA and protein levels, including *AKAP12*, *FOXN3*, *FOXO1*, and *LATS2* (Figures 6C and 6D). In contrast, LNC-HC knockdown decreased the expression of these genes (Figures 6E and 6F). In LO2 cells, LNC-HC increased four genes, including *AKAP12*, *DYRK2*, *FOXO1*, and *LATS2* (Figures S3C and S3D), while LNC-HC knockdown decreased these four genes (Figures S3E and S3F). To further elucidate the ceRNA regulation, we

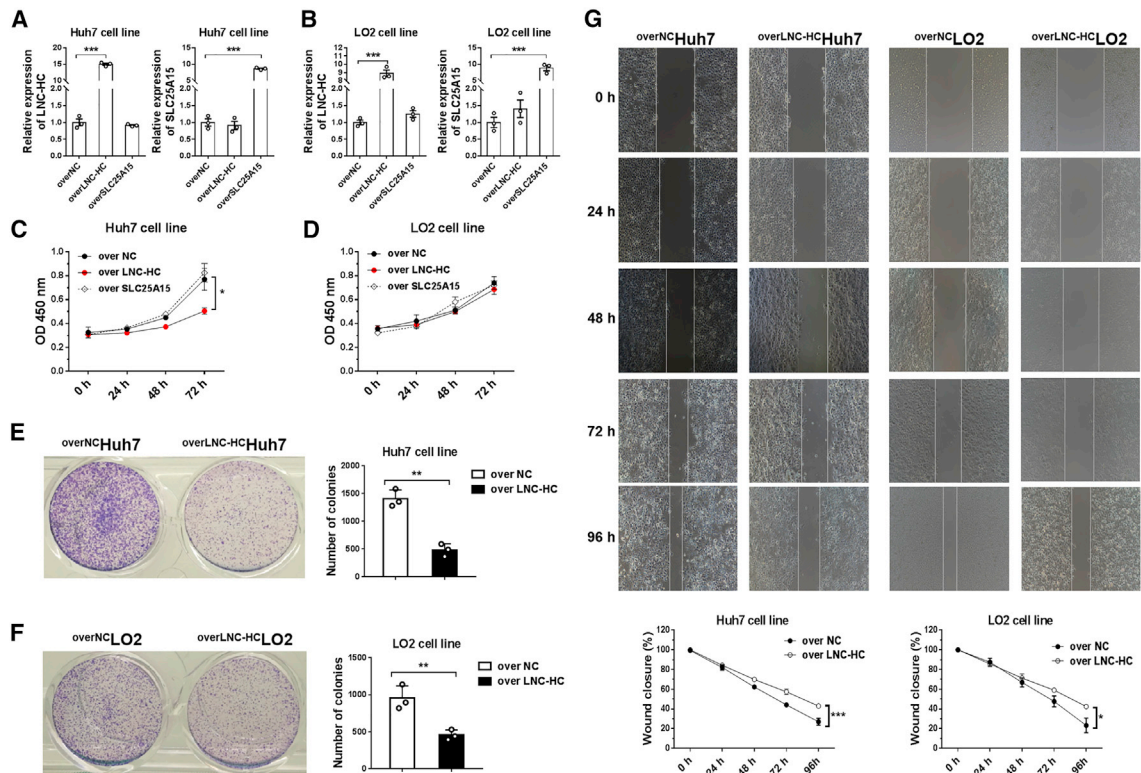


**Figure 3. LNC-HC Suppressed Cell Proliferation and Migration**

(A) Quantitative real-time PCR detection of *LNC-HC* and *SLC25A15* expression in *LNC-HC* or *SLC25A15* stably overexpressing Huh7 cells. (B) Quantitative real-time PCR detection of *LNC-HC* and *SLC25A15* in the indicated stably overexpressing LO2 cells. (C) MTT assay measurement of the proliferation of the indicated Huh7 cells at different time points (0, 24, 48, and 72 h). (D) MTT measurement of the proliferation of LO2 cells at different time points (0, 24, 48, and 72 h). (E) Colony formation of *overNC*Huh7 and *overLNC-HC*Huh7 cells (left) and quantification histogram (right). (F) Colony formation of *overNC*LO2 and *overLNC-HC*LO2 cells (left) and quantification histogram (right). (G) Detection of the migration of *overNC*Huh7/LO2 and *overLNC-HC*Huh7/LO2 cells by using a wound healing assay (up) and quantification histogram (low). *ACTB* was utilized for normalization in the quantitative real-time PCR. \* $p < 0.05$ , \*\* $p < 0.01$ , \*\*\* $p < 0.001$ . Values are expressed as the means  $\pm$  SEM.

overexpressed *miR-183* and *LNC-HC* expression in cells. The results showed that *LNC-HC* could completely rescue the suppressive effect of *miR-183* on expression of the four genes Huh7 cells, including *AKAP12*, *FOXN3*, *FOXO1*, and *LATS2* (Figures 6G and 6H). Meanwhile, the expressions of four genes, including *AKAP12*, *DYRK2*, *FOXO1*, and *LATS2*, were rescued by *LNC-HC* overexpression in LO2 cells (Figures S3G and S3H).

To further check the effect of *LNC-HC* and *miR-183* target genes on Huh7 cell proliferation, an MTT assay and colony formation and wound healing experiments were performed under the condition of *LNC-HC* overexpression and knockdown of indicated genes, including *AKAP12*, *FOXN3*, *FOXO1*, and *LATS2*. Each gene could be significantly knocked down by small interfering RNAs (siRNAs) (Figure S4A). MTT results showed that knockdown of *FOXN3* and *LATS2* could significantly counteract the suppression effect of *LNC-HC* on the proliferation of Huh7 cells; knockdown of *AKAP12* and *FOXO1* has no obvious effect on that within 96 h (Figure S4B). Similarly, knockdown of *FOXN3* and *LATS2* increased the number of colony formations as compared with the *LNC-HC* overexpression group

(Figures S5A and S5B). A wound healing assay suggested that only *FOXN3* knockdown strongly suppressed the metastasis of Huh7 cells under *LNC-HC* overexpression, while the other three genes showed no obvious effect within 96 h (Figures S6A and S6B). These results doubly confirmed that *LNC-HC* suppresses HCC cell proliferation; in addition, they suggested the critical roles of *LNC-HC*/*miR-183*/*FOXN3* and *LATS2* pathways on cell proliferation.

To verify the association between *LNC-HC* and its target genes, we further checked their expressions in hepatic tissues from HCC patients. These genes were all significantly decreased in tumors compared to those in adjacent tissues (Figures 6I and S7A). The Kaplan-Meier analysis showed that high mRNA level of *AKAP12*, *FOXN3*, *FOXO1*, and *LATS2* associated with better patients median overall survival in patients with liver cancer (Figure 6J); however, a high level of *DYRK2* mRNA indicated poor patient survival (Figure S7B). With regard to the correlation between the expression of *LNC-HC* and its target genes, three genes (*AKAP12*, *FOXN3*, and *LATS2*) were significantly correlated with *LNC-HC* in hepatic tumors; only *LATS2* was significantly correlated with *LNC-HC* both in tumor

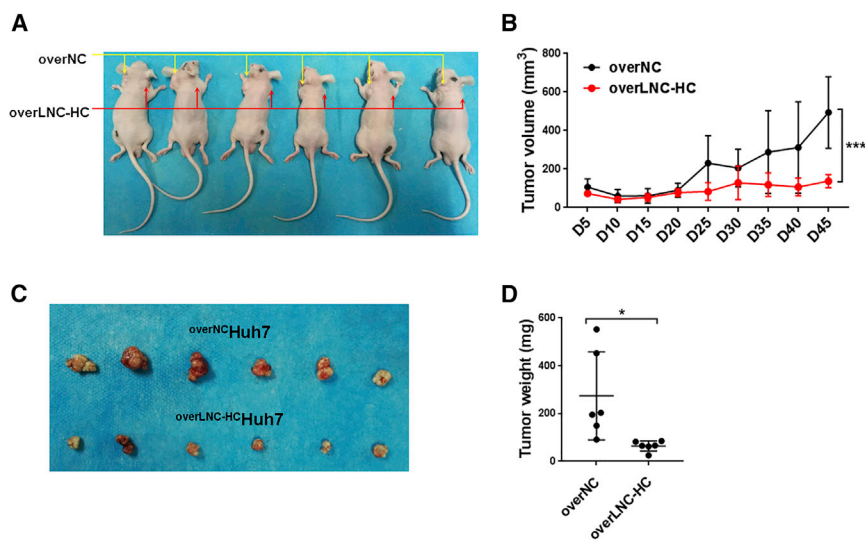


**Figure 4. LNC-HC Inhibited Tumor Growth in a Xenograft Mouse Model**

(A) BALB/c nude mice (aged 4 weeks, male,  $n = 6$ ) were subcutaneously injected with  $5 \times 10^6$   $^{overNC}$ Huh7 (left side) or  $^{overLNC-HC}$ Huh7 cells (right side) per mouse. (B) Tumor volumes were measured every 5 days from day 5 to day 45. On day 45, the mice were sacrificed. (C and D) The tumors from model mice were collected (C) and weighed (D). \* $p < 0.05$ , \*\*\* $p < 0.001$ . Values are expressed as the means  $\pm$  SEM.

and in adjacent tissues. *AKAP12* and *LATS2* showed a significant correlation with *LNC-HC* in all samples containing tumor, adjacent tissues, and normal tissues (Table 2). These findings verified that *LNC-HC* and *miR-183* regulate downstream tumor repressors through a ceRNA pattern both *in vitro* and *in vivo*.

## DISCUSSION

In the current study, we identified a novel human lncRNA, *LNC-HC*, that is the human homolog of rat *lnc-HC*. We verified its function as an inhibitor of HCC cell growth *in vitro* and its role as a tumor suppressor *in vivo*. Mechanistically, *LNC-HC* upregulates the expression of a cluster of tumor repressors, including *AKAP12*, *DYRK2*, *FOXN3*, *FOXO1*, and *LATS2*, by sequestering *miR-183* as a ceRNA.

*LNC-HC* is the human homolog of rat *lnc-HC* and possesses a high degree of synteny, indicating it has a good conservation. SMART RACE and northern blotting confirmed that *LNC-HC* is a novel transcript of 1,063 nt. Both bioinformatics analysis and FLAG/EGFP-tag fusion protein expression indicated that *LNC-HC* has no protein coding potential. These results confirmed that *LNC-HC* functions as a lncRNA.

We further explored the function of human *LNC-HC* in HCC development. *LNC-HC* is significantly decreased in HCC hepatic tumors as well as in three types of HCC cell lines, including Huh7, Hep3B, and Skhep1. The mRNA expression of *SLC25A15*, a protein-encoding gene that overlaps with *LNC-HC*, was likewise significantly decreased in tumor tissues. However, expression of the two genes demonstrated a lack of correlation in HCC cells and HCC tumors, suggesting their independent expression patterns under these two conditions and different pathways in modulating cancer pathology; in addition, the two genes showed strong correlation in adjacent tissues, suggesting their potential cooperation in regulating tumorigenesis and indicating the aberrant gene profile presented in adjacent tissues. Although there

is no significance regarding the correlation between *LNC-HC* expression and clinicopathological characteristics ( $p > 0.05$ ), a low level of *LNC-HC* was clearly correlated with TNM stage and tumor size to a certain extent. The correlation tends to be significant with a bigger sample size. We further focused on *LNC-HC* by excluding the effects of *SLC25A15*. We constructed *LNC-HC*-overexpressing stable cells and utilized *SLC25A15* overexpression as a control. The MTT assay showed that  $^{overLNC-HC}$ Huh7 cells showed a slower proliferation rate over 72 h compared with  $^{overNC}$ Huh7 and  $^{overSLC25A15}$ Huh7 cells; however, no detectable change in proliferation was identified in LO2 cells. This might be because LO2 cells are a normal hepatocyte cell line with an increased baseline of *LNC-HC* level and thus have a normal proliferation rate. Nonetheless, during a longer cultivation, the growth difference between  $^{overNC}$ LO2 and  $^{overLNC-HC}$ LO2 cells was much more obvious, as indicated by the colony formation assay. In addition to the *in vitro* evidence, an *in vivo* mouse model further established the antitumor effect of *LNC-HC*.

The ceRNA hypothesis was proposed by Salmena et al.<sup>50</sup> in 2011. Several lines of evidence in this field have shown the role of ceRNA in the fine-tuning of regulatory pathways; nonetheless, only a few studies have reported the role of ceRNAs in liver cancer pathology.<sup>51–56</sup> A full understanding of the ceRNAs involved in HCC, including those formed by lncRNAs and microRNAs, could provide new insights and new therapeutic targets for HCC. In our study, *miR-183* was identified as the coregulator of *LNC-HC*. In agreement with previous studies, *miR-183* expression was dramatically increased in HCC tumor tissues and is considered an oncomiRNA.<sup>29,46,49,57–60</sup> Interestingly, we also identified two microRNAs, *miR-4482* and *miR-10527*, that were predicted to target *LNC-HC* and were significantly reduced in HCC tumors. Previous studies have not reported these two microRNAs in relationship to cancer development. In Huh7 cells, *miR-183* significantly promoted cell growth; *LNC-HC* overexpression strongly eliminated this effect. In LO2 cells, *LNC-HC* overexpression resulted in no changes in cell proliferation compared with the control group during 72 h; however, it significantly suppressed cell proliferation compared with the *miR-183*-transfected  $^{overNC}$ LO2 group. This difference between Huh7 and LO2 cells may due to the fact that the LO2 cells had a slower proliferation rate and transformed into a

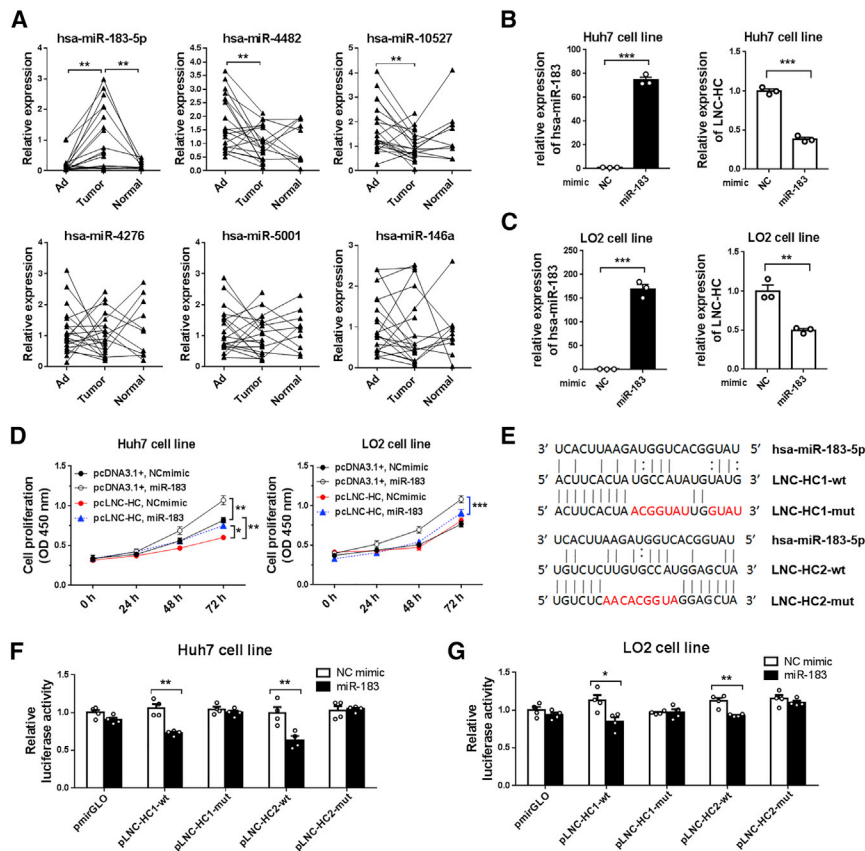


**Figure 5. miR-183 Directly Interacted with LNC-HC**

(A) Quantitative real-time PCR detection of the expression of the indicated microRNAs in hepatic tumor samples. (B) Quantitative real-time PCR detection of *miR-183* and *LNC-HC* expression in Huh7 cells transfected with the negative control mimic (NC, 50 nM) or *miR-183* mimic (*miR-183*, 50 nM) for 24 h. (C) Quantitative real-time PCR detection of *miR-183* and *LNC-HC* expression in LO2 cells transfected with the NC mimic (50 nM) or *miR-183* mimic (50 nM) for 24 h. (D) MTT assay of the cell proliferation under *LNC-HC* or *miR-183* overexpression. (E) Schematic diagram of wild-type and site-directed mutant of the *miR-183* binding sites 1 and 2 within the *LNC-HC* sequence. (F) Dual-luciferase reporter gene assay of the Huh7 cells cotransfected with pLNC-HC1/2-WT/mut and NC/*miR-183* mimic. (G) Luciferase activity of LO2 cells cotransfected with pLNC-HC1/2-WT/mut and NC/*miR-183* mimic. \* $p < 0.05$ , \*\* $p < 0.01$ , \*\*\* $p < 0.001$ . Values are expressed as the means  $\pm$  SEM.

carcinoma cell type when *miR-183* was overexpressed; under this condition, the tumor suppressor function of *LNC-HC* was obvious.

Furthermore, we also explored the *LNC-HC/miR-183* ceRNA pathway in regulating downstream tumor repressors. As a novel gene, it is difficult to analyze the correlation between *LNC-HC* expression and patient survival with liver cancer. We thereupon checked its target genes, including *AKAP12*, *DYRK2*, *FOXN3*, *FOXO1*, and *LATS2*, and the HCC patient survival rate by using the public RNA sequencing (RNA-seq) database Kaplan-Meier Plotter. Except for *DYRK2*, the high mRNA levels of *AKAP12*, *FOXN3*, *FOXO1*, and *LATS2* predicted the longer patient survival. This is in accordance with the results shown in Figure 6, *LNC-HC/miR-183* coregulate the four genes in Huh7 cells; *DYRK2* could be controlled only in LO2 cells. The discrepancy of *DYRK2* suggests a potential variation during cancer pathogenesis. Supposing that *DYRK2* overexpression is a compensatory effect induced by a high degree of malignancy, it could be explained that decreased *DYRK2* predicts longer patient survival. However, one existing study reported that depletion of *DYRK2* promoted HCC cell proliferation.<sup>61</sup> This group further showed that a low expression of *DYRK2* predicted a poor prognosis for HCC patients ( $n = 86$ ). Due to the above contradiction, more studies need to be conducted to detail the function and expression pattern of *DYRK2* during HCC pathogenesis. *AKAP12* and *FOXN3* have

been reported to be decreased in HCC tissues compared to adjacent hepatic tissues and to function as tumor suppressors.<sup>20,62–64</sup> In our study, *AKAP12* and *FOXN3* were verified to be correlated with *LNC-HC* expression in HCC tumors but not in paired-adjacent and normal samples. These observations suggested that the function of *LNC-HC* was different under different conditions, such as normal and carcinogenic treatments. *LATS2* is an influential molecule with strong antitumor effects. It play roles in mitochondrial function and the Wnt/ $\beta$ -catenin pathway,<sup>65</sup> AMPK-Mfn2 pathway,<sup>66</sup> EMT,<sup>67,68</sup> Hippo pathway<sup>69,70</sup> and the YAP/TAZ system.<sup>71–73</sup> Here, *LATS2* was strongly correlated with *LNC-HC* not only in tumors and adjacent liver tissues, but also in all samples containing tumor, adjacent tissue, and normal liver tissue. When combined, the results of correlation analysis with the MTT, colony formation, and wound healing assays under *LNC-HC* overexpression and target gene knock-down, it could be concluded that the *LNC-HC/miR-183/FOXN3* and *LATS2* pathways play a vital role in HCC cell proliferation and HCC pathology.

Overall, we identified *LNC-HC* as a novel human lncRNA and described its antitumor function in HCC. The identification of *LNC-HC* not only reveals new regulatory pathways important for understanding HCC pathology, but it also provides new insights into therapeutic possibilities for the prevention and treatment of HCC.

## MATERIALS AND METHODS

### SMART RACE

The human homologous nucleotide fragment of rat *lnc-HC* was obtained through a BLAST search of the UCSC database. Then, 5'- and 3'-RACE of *LNC-HC* were conducted using the BD SMART RACE cDNA amplification kit (Clontech Laboratories, Mountain View, CA,

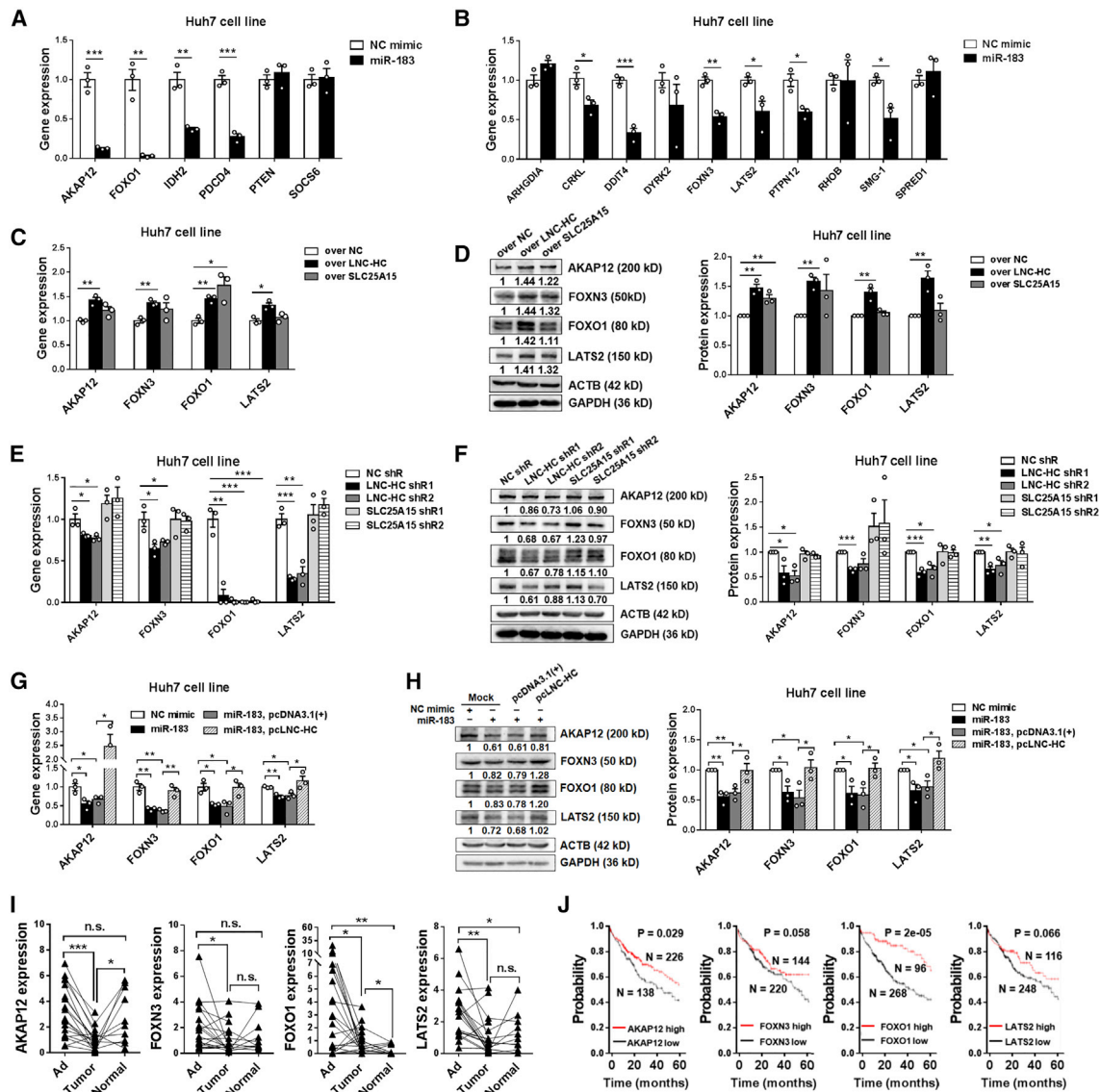


**Figure 6. LNC-HC and miR-183 Coregulated Downstream Tumor Repressor Expression as a ceRNA Pattern**

(A and B) Quantitative real-time PCR analysis of indicated expression of genes in NC/*miR-183* mimic-transfected Huh7 cells. (A) Genes already verified as *miR-183* targets. (B) Genes predicted to be targets of *miR-183*. (C) Quantitative real-time PCR detection of gene expression in *overLNC-HC* Huh7 and *overSLC25A15* Huh7 cells. (D) Western blotting analysis of the indicated gene expression in *overLNC-HC* Huh7 and *overSLC25A15* Huh7 cells (left) and quantification histograms (right). (E) Quantitative real-time PCR detection of *miR-183*-targeted gene expression in *LNC-HC* or *SLC25A15* knockdown Huh7 cells. (F) Western blotting analysis of indicated gene expression in *LNC-HC* or *SLC25A15* knockdown Huh7 cells (left) and quantification histogram (right). (G) Quantitative real-time PCR detection of indicated genes in Huh7 cells transfected with NC/*miR-183* mimic and pcDNA3.1+/pcLNC-HC for 24 h. (H) Western blotting analysis of indicated gene expression in Huh7 cells transfected with NC/*miR-183* mimic and pcDNA3.1+/pcLNC-HC (left) and quantification histogram (right). (I) Quantitative real-time PCR detection of *LNC-HC*-targeted genes in hepatic tumor samples. (J) Kaplan-Meier plots of median overall survival data for patients with liver cancer (n = 364) by using Kaplan-Meier Plotter. Western blotting shows one representative result and quantitative data from three independent experiments. ACTB was the loading control in the western blotting assay. \**p* < 0.05, \*\**p* < 0.01, \*\*\**p* < 0.001. Values are expressed as the means ± SEM.

USA) according to the manufacturer's instructions. The primers used for 5'-RACE of *LNC-HC* were 5'-CTCCCAACCTAAGTTTCC GTTCCTCA-3' (5-GSP) and 5'-CGTTCCTCATTTCCACTTGCCT CAGA-3' (5-NGSP). The primers used for 3'-RACE of *LNC-HC* were 5'-AATCACAGAGCCAGAAGCCAGAGGG-3' (3-GSP) and 5'-GAGGCAAGTGGAAATGAGGAACGG-3' (3-NGSP).

### Bioinformatics Analysis

The ORF prediction of *LNC-HC* was conducted using the ORF Finder online software (<https://www.ncbi.nlm.nih.gov/orffinder/>). The predicted *LNC-HC* ORFs are depicted in Table S2. The conserved protein domains were verified by comparison to the predicted *LNC-HC* ORFs obtained from a protein BLAST search

**Table 2. Correlation between *LNC-HC* and Target Genes in Hepatic Tumors from Patients with HCC**

Gene	Correlation Analysis between <i>LNC-HC</i> and Target Genes Expression							
	Tumor		Adjacent		Normal		All Samples	
	r Value	p Value	r Value	p Value	r Value	p Value	r Value	p Value
<i>AKAP12</i>	0.5889	0.0063**	0.2208	0.3495	0.1634	0.6520	0.385	0.0058**
<i>DYRK2</i>	0.3774	0.1009	-0.0338	0.8875	0.5823	0.0774	0.2357	0.0995
<i>FOXN3</i>	0.5045	0.0233*	-0.0361	0.8798	0.4152	0.2328	0.1822	0.2054
<i>FOXO1</i>	0.2604	0.2675	0.2017	0.3939	-0.5475	0.1014	0.276	0.0524
<i>LATS2</i>	0.5376	0.0145*	0.5278	0.0168*	0.0013	0.9972	0.5121	0.0001***

\*p < 0.05, \*\*p < 0.01, \*\*\*p < 0.001.

(<https://blast.ncbi.nlm.nih.gov/Blast.cgi>) of the nonredundant protein sequences (nr) and reference proteins (refseq\_protein) databases. The translation potential of *LNC-HC* was determined with a coding potential calculator (<http://cpc2.cbi.pku.edu.cn/>).

#### Northern Blotting

Northern blotting analysis was performed by using total RNA (30 µg) from the LO2 cell line, with digoxigenin (DIG)-labeling *SLC25A15*-probe or *LNC-HC*-probe. Detection was conducted with the DIG-High Prime DNA labeling and detection starter kit II (Roche, Basel, Switzerland), according to the manufacturer's instructions. The primers used for the *SLC25A15* DIG-labeling probe are 5'-TCCAA TCCTGCTATCCAGGC-3' and 5'-CCGGCTCAGTTCATAGCC AC-3', and for *LNC-HC* the DIG-labeling probe are 5'-AGTGTTCCT AAGCAGCCTGT-3' and 5'-TTCCTCATTCCACTTGCC-3'.

#### Construction of EGFP/FLAG Fusion Protein Expression Vectors and Protein Expression Assay

The C-terminal EGFP and FLAG tag were inserted into the pcDNA3.1+ vector between the *EcoRI* and *XhoI* restriction sites (Figure S1). Then, the predicted ORF1–3 of *LNC-HC* (from the transcription start site to the end of ORFs without a stop codon) was inserted into the pcDNA3.1-EGFP/FLAG vector between the *BamHI* and *EcoRI* sites. The first exon sequence of protein-coding gene *ACTB* (171 bp, 48 bp before the ATG start codon and without a stop codon) was the control of the protein coding gene. *Lnc-DC* (621 bp, full-length sequence, without a stop codon) was the control of lncRNAs. The primers for amplifying target sequence are shown in Table S3. These vectors were transfected into LO2 cells separately with Lipofectamine 2000 (Invitrogen, Waltham, MA, USA), according to the manufacturer's instructions. After 48 h, FLAG-tag plasmid-transfected cells were collected for immunoblotting, whereas EGFP-tag plasmid-transfected cells were visualized by fluorescence microscopy (Olympus, Tokyo, Japan). To detect the FLAG-tag fusion protein expression, cell lysates were loaded in nitrocellulose (NC) membrane at the indicated level (2, 1.75, 1.5, 1.25, 1, 0.75, and 0.5 µg). GAPDH (10 µg of protein from each group of cells) was the loading control. Mouse anti-FLAG antibody (CMCTAG, Shanghai, China) and mouse anti-GAPDH antibody (CMCTAG, Shanghai, China) were the primary antibodies.

#### Clinical Samples and Cell Lines

Twenty hepatic tumor tissues, 20 paired adjacent non-tumor tissues, and 10 paired normal tissues were obtained from patients with HCC who underwent surgical treatment at The First Affiliated Hospital of Xi'an Jiaotong University (Xi'an, China). Adjacent non-tumor tissues were defined as tissues >1 cm and <5 cm from the tumor boundary. Normal tissues were defined as tissues >5 cm from the tumor boundary. Signed informed consents were collected and the study was approved by the Ethics Committee of The First Affiliated Hospital of Xi'an Jiaotong University. LO2 cells were maintained in RPMI 1640 medium (HyClone, South Logan, UT, USA) containing 10% fetal bovine serum (FBS) (ExCell Bio, Shanghai, China). Huh7 cells were maintained in DMEM high-glucose medium (HyClone, South Logan, UT, USA) supplemented with 10% FBS (ExCell Bio, Shanghai, China).

#### RNA Isolation and Quantitative Real-Time PCR

Total RNA was isolated from stored HCC liver samples, LO2 cells, and Huh7 cells. RNA was extracted using TRIzol reagent (Invitrogen, Waltham, MA, USA). The extraction was performed with the chloroform-isopropanol method. RNA quality and concentration were measured using a NanoDrop instrument. cDNAs were generated by the reverse transcription of mRNAs with 5 µg of total RNA per sample using the RevertAid first-strand cDNA synthesis kit (Thermo Fisher Scientific, Waltham, MA, USA). The microRNA cDNAs were reverse transcribed with 2 µg of total RNA per sample using a Mir-X miRNA qRT-PCR SYBR kit (Clontech Laboratories, Mountain View, CA, USA). Quantitative real-time PCR was performed using SYBR Green qPCR master mix (Roche, Basel, Switzerland) in an Agilent Mx3005P instrument. Primer information for the mRNA quantitative real-time PCR is shown in Table S4. Primer information for the microRNA quantitative real-time PCR is shown in Table S5.

#### Western Blotting

Protein was isolated from cells by using cell lysis buffer (Beyotime Biotechnology, Shanghai, China). Protein from different cells were separated by 8% SDS-PAGE gel and transferred onto a polyvinylidene fluoride (PVDF) membrane (Bio-Rad, Hercules, CA, USA) according to the standard process. Protein expression was analyzed by using rabbit anti-ACTB antibody (Santa Cruz Biotechnology, Shanghai,

China, 1:500), mouse anti-GAPDH antibody (CMCTAG, Shanghai, China), rabbit anti-AKAP12 antibody (Proteintech, Wuhan, Hubei, China, 1:1,000), mouse anti-DYRK2 antibody (R&D Systems, Minneapolis, MN, USA, 1:1,000), rabbit anti-FOXN3 antibody (Abcam, Cambridge, MA, USA, 1:1,000), rabbit anti-FOXO1 antibody (Proteintech, Wuhan, Hubei, China, 1:1,000), and rabbit anti-LATS2 antibody (Proteintech, Wuhan, Hubei, China, 1:1,000).

### Gene Overexpression and Knockdown

The expression vectors were constructed first. Full-length *LNC-HC* was obtained by PCR with PrimeSTAR GXL DNA polymerase (Takara Bio, Beijing, China) and inserted into the pcDNA3.1+ vector between the *EcoRI* and *XhoI* sites to obtain pcLNC-HC; the *SLC25A15* coding region was inserted into the pcDNA3.1+ vector between *HindIII* and *BamHI* sites to obtain pcSLC25A15. The primers are shown in Table S6. For gene knockdown, short hairpin RNAs (shRNAs) for *LNC-HC* and *SLC25A15* knockdown were ordered from GenePharma (Shanghai, China). The target sequences of the *LNC-HC* shRNAs and the *SLC25A15* shRNAs are shown in Table S6. After the transfection of pcDNA3.1+, pcLNC-HC, pcSLC25A15, NC shRNAs, *LNC-HC* shRNAs, and *SLC25A15* shRNAs using Lipofectamine 2000 (Invitrogen, Waltham, CA, USA) for 24 h, LO2 and Huh7 cells were treated with G418 (600 µg/mL in LO2 and 800 µg/mL in Huh7) for a period of 30 days to select the stable cell lines <sup>overNC</sup>LO2/Huh7, <sup>overLNC-HC</sup>LO2/Huh7, <sup>overSLC25A15</sup>LO2/Huh7, <sup>NCshR</sup>LO2/Huh7, <sup>LNC-HCshR</sup>LO2/Huh7, and <sup>SLC25A15shR</sup>LO2/Huh7, respectively.

### Cell Proliferation Assay

An MTT assay was used to measure cell proliferation. In detail,  $1 \times 10^4$  Huh7 or LO2 cells were seeded per well in a 96-well plate. The cells were transfected with the NC mimic (50 nM) or *miR-183* mimic (50 nM) by using Lipofectamine RNA iMAX reagent (Invitrogen, Waltham, CA, USA) and the pcDNA3.1+ or pcLNC-HC vector by using Lipofectamine 2000 reagent (Invitrogen, Waltham, CA, USA) according to the manufacturer's instructions. To check the cooperative effect of *LNC-HC* overexpression and knockdown of its target genes, Huh7 cells were transfected with pcDNA3.1+ or pcLNC-HC vector and NC siRNA (50 nM) or the indicated siRNA (50 nM). At different time points (0, 24, 48, and 72 h) the cells were incubated with 0.5 mg/mL MTT solution at 37°C for 4 h. Then, the culture medium was changed to DMSO (150 µL per well). The optical absorbance was measured at a wavelength of 450 nm. The sequence information for the *miR-183* mimic, NC mimic, siRNAs targeting *AKAP12*, *FOXN3*, *FOXO1*, and *LATS2* and NC siRNA are shown in Table S7. The siRNAs were ordered from Genepharma (Shanghai, China).

### Mouse Xenograft Tumor Model

Animal experiments were approved by the Institutional Animal Ethics Committee of the Xi'an Jiaotong University School of Medicine (permission ID XJ2006Y039; Xi'an Jiaotong University, Xi'an, China) and were conducted in accordance with the European Communities Council Directive 2010/63/EU for the protection of animals used for scientific purposes. Male BALB/c nude mice ( $n = 6$ , aged 4 weeks)

were ordered from the Medical Experimental Animal Center, Xi'an Jiaotong University. For the xenograft tumor model,  $5 \times 10^6$  <sup>overNC</sup>Huh7 or <sup>overLNC-HC</sup>Huh7 cells were subcutaneously injected into the left or right flanks of nude mice on day 1. After 5 days, the tumor volume and body weight were detected every 5 days. On day 45, the mice were sacrificed, and the tumors were collected and measured.

### Dual-Luciferase Reporter Gene Assay

The *LNC-HC* DNA fragments targeted by *hsa-miR-183-5p* (wild-type and mutant) were ordered from Sangon Biotech (Shanghai, China). They were inserted into the pmirGLO vector between the *NheI* and *XhoI* sites to generate pLNC-HC1-WT, pLNC-HC1-mut, pLNC-HC2-WT, and pLNC-HC2-mut. LO2 and Huh7 cells were seeded into 48-well plates and cotransfected with different pLNC-HC-target plasmids (100 ng) and NC/*miR-183* mimic (50 nM) for 24 h. The relative luciferase activity of each cell group was measured using the Dual-luciferase reporter assay system (Promega, Madison, WI, USA) according to the manufacturer's instructions.

### Survival Analysis

The effects of *AKAP12*, *DYRK2*, *FOXN3*, *FOXO1*, and *LATS2* on the overall survival of patients with liver cancer ( $n = 364$ ) were analyzed by using the online RNA-seq database Kaplan-Meier Plotter (<http://kmplot.com/analysis/>).<sup>74</sup>

### Statistical Analysis

Quantitative data were expressed as the means  $\pm$  SEM. The statistical analysis of the differences between groups was conducted by using an unpaired Student's *t* test. The difference in xenograft tumor growth between the <sup>overNC</sup>Huh7 and <sup>overLNC-HC</sup>Huh7 injection groups was analyzed by two-way ANOVA. The Fisher's exact test was performed to compare the association between *LNC-HC* expression and clinical parameters. \* $p < 0.05$ , \*\* $p < 0.01$ , and \*\*\* $p < 0.001$  were considered statistically significant.

### SUPPLEMENTAL INFORMATION

Supplemental Information can be found online at <https://doi.org/10.1016/j.omtn.2020.03.008>.

### AUTHOR CONTRIBUTIONS

Study design: X.L. and S.L. Analysis and interpretation of the data: X.L. Drafting of the manuscript: X.L. and S.L. Critical revision of the manuscript: X.L., S.L. and E.K.O. Obtained funding: X.L. and L.L. Performance of the experiments: X.L., N.W., L.W., and X.D. Collection of the clinical samples: K.Q. and H.L. Preparation and assistant work: J.R., B.W., L.L., and Q.N. Necessary technical guides: D.G., S.C., J.M., and D.L.

### CONFLICTS OF INTEREST

The authors declare no competing interests.

### ACKNOWLEDGMENTS

This project was supported by the National Natural Science Foundation of China (81600679 to X.L. and 31801083 to L.L.); the China

Postdoctoral Science Foundation (2016M592778 to X.L.); the Fundamental Research Funds for the Central Universities (xjj2017051 to X.L.); and the Shaanxi Postdoctoral Science Foundation (2016BSHEDZZ98 to X.L.).

## REFERENCES

- Fu, J., and Wang, H. (2018). Precision diagnosis and treatment of liver cancer in China. *Cancer Lett.* 412, 283–288.
- Cronin, K.A., Lake, A.J., Scott, S., Sherman, R.L., Noone, A.M., Howlander, N., Henley, S.J., Anderson, R.N., Firth, A.U., Ma, J., et al. (2018). Annual Report to the Nation on the Status of Cancer, part I: national cancer statistics. *Cancer* 124, 2785–2800.
- Chen, W., Zheng, R., Baade, P.D., Zhang, S., Zeng, H., Bray, F., Jemal, A., Yu, X.Q., and He, J. (2016). Cancer statistics in China, 2015. *CA Cancer J. Clin.* 66, 115–132.
- Nelson, B.R., Makarewich, C.A., Anderson, D.M., Winders, B.R., Troupes, C.D., Wu, F., Reese, A.L., McAnally, J.R., Chen, X., Kavalali, E.T., et al. (2016). A peptide encoded by a transcript annotated as long noncoding RNA enhances SERCA activity in muscle. *Science* 351, 271–275.
- Huang, J.Z., Chen, M., Chen, D., Gao, X.C., Zhu, S., Huang, H., Hu, M., Zhu, H., and Yan, G.R. (2017). A peptide encoded by a putative lncRNA HOXB-AS3 suppresses colon cancer growth. *Mol. Cell* 68, 171–184.e6.
- Chen, Z.Z., Huang, L., Wu, Y.H., Zhai, W.J., Zhu, P.P., and Gao, Y.F. (2016). *LncSox4* promotes the self-renewal of liver tumour-initiating cells through Stat3-mediated Sox4 expression. *Nat. Commun.* 7, 12598.
- Gupta, R.A., Shah, N., Wang, K.C., Kim, J., Horlings, H.M., Wong, D.J., Tsai, M.C., Hung, T., Argani, P., Rinn, J.L., et al. (2010). Long non-coding RNA HOTAIR reprograms chromatin state to promote cancer metastasis. *Nature* 464, 1071–1076.
- Yuan, S.X., Wang, J., Yang, F., Tao, Q.F., Zhang, J., Wang, L.L., Yang, Y., Liu, H., Wang, Z.G., Xu, Q.G., et al. (2016). Long noncoding RNA *DANCR* increases stemness features of hepatocellular carcinoma by derepression of *CTNNB1*. *Hepatology* 63, 499–511.
- Cao, C., Sun, J., Zhang, D., Guo, X., Xie, L., Li, X., Wu, D., and Liu, L. (2015). The long intergenic noncoding RNA *UF1*, a target of microRNA 34a, interacts with the mRNA stabilizing protein HuR to increase levels of  $\beta$ -catenin in HCC cells. *Gastroenterology* 148, 415–426.e18.
- Quagliata, L., Matter, M.S., Piscuoglio, S., Arabi, L., Ruiz, C., Procino, A., Kovac, M., Moretti, F., Makowska, Z., Boldanova, T., et al. (2014). Long noncoding RNA *HOTTIP/HOXA13* expression is associated with disease progression and predicts outcome in hepatocellular carcinoma patients. *Hepatology* 59, 911–923.
- Wang, F., Yuan, J.H., Wang, S.B., Yang, F., Yuan, S.X., Ye, C., Yang, N., Zhou, W.P., Li, W.L., Li, W., and Sun, S.H. (2014). Oncofetal long noncoding RNA *PVT1* promotes proliferation and stem cell-like property of hepatocellular carcinoma cells by stabilizing *NOP2*. *Hepatology* 60, 1278–1290.
- Zhu, P., Wang, Y., Huang, G., Ye, B., Liu, B., Wu, J., Du, Y., He, L., and Fan, Z. (2016). *lnc- $\beta$ -Catm* elicits *EZH2*-dependent  $\beta$ -catenin stabilization and sustains liver CSC self-renewal. *Nat. Struct. Mol. Biol.* 23, 631–639.
- Yuan, J.H., Yang, F., Wang, F., Ma, J.Z., Guo, Y.J., Tao, Q.F., Liu, F., Pan, W., Wang, T.T., Zhou, C.C., et al. (2014). A long noncoding RNA activated by TGF- $\beta$  promotes the invasion-metastasis cascade in hepatocellular carcinoma. *Cancer Cell* 25, 666–681.
- Wang, J., Liu, X., Wu, H., Ni, P., Gu, Z., Qiao, Y., Chen, N., Sun, F., and Fan, Q. (2010). CREB up-regulates long non-coding RNA, *HULC* expression through interaction with microRNA-372 in liver cancer. *Nucleic Acids Res.* 38, 5366–5383.
- Li, T., Xie, J., Shen, C., Cheng, D., Shi, Y., Wu, Z., Deng, X., Chen, H., Shen, B., Peng, C., et al. (2015). Amplification of long noncoding RNA *ZFAS1* promotes metastasis in hepatocellular carcinoma. *Cancer Res.* 75, 3181–3191.
- Lan, X., Yan, J., Ren, J., Zhong, B., Li, J., Li, Y., Liu, L., Yi, J., Sun, Q., Yang, X., et al. (2016). A novel long noncoding RNA *lnc-HC* binds *hnRNP2B1* to regulate expressions of *Cyp7a1* and *Abca1* in hepatocytic cholesterol metabolism. *Hepatology* 64, 58–72.
- Lan, X., Wu, L., Wu, N., Chen, Q., Li, Y., Du, X., Wei, C., Feng, L., Li, Y., Osoro, E.K., et al. (2019). Long noncoding RNA *lnc-HC* regulates PPAR $\gamma$ -mediated hepatic lipid metabolism through *miR-130b-3p*. *Mol. Ther. Nucleic Acids* 18, 954–965.
- Zhang, J., Piao, H.Y., Guo, S., Wang, Y., Zhang, T., Zheng, Z.C., and Zhao, Y. (2020). *LINC00163* inhibits the invasion and metastasis of gastric cancer cells as a ceRNA by sponging *miR-183* to regulate the expression of *AKAP12*. *Int. J. Clin. Oncol.* Published online January 1, 2020. <https://doi.org/10.1007/s10147-019-01604-w>.
- Kang, J., Kim, W., Lee, S., Kwon, D., Chun, J., Son, B., Kim, E., Lee, J.M., Youn, H., and Youn, B. (2017). *TFAP2C* promotes lung tumorigenesis and aggressiveness through *miR-183*- and *miR-33a*-mediated cell cycle regulation. *Oncogene* 36, 1585–1596.
- Goeppert, B., Schmezer, P., Dutruel, C., Oakes, C., Renner, M., Breinig, M., Warth, A., Vogel, M.N., Mittelbronn, M., Mehrabi, A., et al. (2010). Down-regulation of tumor suppressor A kinase anchor protein 12 in human hepatocarcinogenesis by epigenetic mechanisms. *Hepatology* 52, 2023–2033.
- Zhou, L., Su, X., Li, B., Chu, C., Sun, H., Zhang, N., Han, B., Li, C., Zou, B., Niu, Y., and Zhang, R. (2019). PM2.5 exposure impairs sperm quality through testicular damage dependent on *NALP3* inflammasome and *miR-183/96/182* cluster targeting *FOXO1* in mouse. *Ecotoxicol. Environ. Saf.* 169, 551–563.
- Suzuki, R., Amatya, V.J., Kushitani, K., Kai, Y., Kambara, T., and Takeshima, Y. (2018). *miR-182* and *miR-183* promote cell proliferation and invasion by targeting *FOXO1* in mesothelioma. *Front. Oncol.* 8, 446.
- Fang, Q., Sang, L., and Du, S. (2018). Long noncoding RNA *LINC00261* regulates endometrial carcinoma progression by modulating *miRNA/FOXO1* expression. *Cell Biochem. Funct.* 36, 323–330.
- Hou, Y., Fu, L., Li, J., Li, J., Zhao, Y., Luan, Y., Liu, A., Liu, H., Li, X., Zhao, S., and Li, C. (2018). Transcriptome analysis of potential miRNA involved in adipogenic differentiation of C2C12 myoblasts. *Lipids* 53, 375–386.
- Ichiyama, K., Gonzalez-Martin, A., Kim, B.S., Jin, H.Y., Jin, W., Xu, W., Sabouri-Ghomi, M., Xu, S., Zheng, P., Xiao, C., and Dong, C. (2016). The microRNA-183-96-182 cluster promotes T helper 17 cell pathogenicity by negatively regulating transcription factor *Foxo1* expression. *Immunity* 44, 1284–1298.
- Gebremedhn, S., Salilew-Wondim, D., Hoelker, M., Rings, F., Neuhoff, C., Tholen, E., Schellander, K., and Tesfaye, D. (2016). MicroRNA-183-96-182 cluster regulates bovine granulosa cell proliferation and cell cycle transition by coordinately targeting *FOXO1*. *Biol. Reprod.* 94, 127.
- Gebremedhn, S., Salilew-Wondim, D., Ahmad, I., Sahadevan, S., Hossain, M.M., Hoelker, M., Rings, F., Neuhoff, C., Tholen, E., Looft, C., et al. (2015). MicroRNA expression profile in bovine granulosa cells of preovulatory dominant and subordinate follicles during the late follicular phase of the estrous cycle. *PLoS ONE* 10, e0125912.
- Zhang, L., Quan, H., Wang, S., Li, X., and Che, X. (2015). *miR-183* promotes growth of non-small cell lung cancer cells through *FoxO1* inhibition. *Tumour Biol.* 36, 8121–8126.
- Leung, W.K., He, M., Chan, A.W., Law, P.T., and Wong, N. (2015). *Wnt/ $\beta$ -catenin* activates *miR-183/96/182* expression in hepatocellular carcinoma that promotes cell invasion. *Cancer Lett.* 362, 97–105.
- Nozaki, T., and Ohura, K. (2014). Regulation of miRNA during direct reprogramming of dental pulp cells to insulin-producing cells. *Biochem. Biophys. Res. Commun.* 444, 195–198.
- McLoughlin, H.S., Wan, J., Spengler, R.M., Xing, Y., and Davidson, B.L. (2014). Human-specific microRNA regulation of *FOXO1*: implications for microRNA recognition element evolution. *Hum. Mol. Genet.* 23, 2593–2603.
- Tang, H., Bian, Y., Tu, C., Wang, Z., Yu, Z., Liu, Q., Xu, G., Wu, M., and Li, G. (2013). The *miR-183/96/182* cluster regulates oxidative apoptosis and sensitizes cells to chemotherapy in gliomas. *Curr. Cancer Drug Targets* 13, 221–231.
- Xie, L., Ushmorov, A., Leithäuser, F., Guan, H., Steidl, C., Färber, J., Pelzer, C., Vogel, M.J., Maier, H.J., Gascoyne, R.D., et al. (2012). *FOXO1* is a tumor suppressor in classical Hodgkin lymphoma. *Blood* 119, 3503–3511.
- Myatt, S.S., Wang, J., Monteiro, L.J., Christian, M., Ho, K.K., Fusi, L., Dina, R.E., Broens, J.J., Ghaem-Maghani, S., and Lam, E.W. (2010). Definition of microRNAs that repress expression of the tumor suppressor gene *FOXO1* in endometrial cancer. *Cancer Res.* 70, 367–377.
- Wang, X.J., Zhang, D.L., Fu, C., Wei, B.Z., and Li, G.J. (2016). *miR-183* modulates multi-drug resistance in hepatocellular cancer (HCC) cells via *miR-183-IDH2/SOCS6-HIF-1 $\alpha$*  feedback loop. *Eur. Rev. Med. Pharmacol. Sci.* 20, 2020–2027.

36. Tanaka, H., Sasayama, T., Tanaka, K., Nakamizo, S., Nishihara, M., Mizukawa, K., Kohta, M., Koyama, J., Miyake, S., Taniguchi, M., et al. (2013). MicroRNA-183 upregulates HIF-1 $\alpha$  by targeting isocitrate dehydrogenase 2 (IDH2) in glioma cells. *J. Neurooncol.* *111*, 273–283.
37. Vohwinkel, C.U., Lecuona, E., Sun, H., Sommer, N., Vadász, I., Chandel, N.S., and Sznajder, J.I. (2011). Elevated CO<sub>2</sub> levels cause mitochondrial dysfunction and impair cell proliferation. *J. Biol. Chem.* *286*, 37067–37076.
38. Lu, Y.Y., Zeng, Y., Zheng, J.Y., Huang, C.L., and Wang, X.P. (2016). [miR-183 regulates proliferation of SW1990 pancreatic cancer cell line by targeting PDCD4]. *Sichuan Da Xue Xue Bao Yi Xue Ban* *47*, 691–696.
39. Cheng, Y., Xiang, G., Meng, Y., and Dong, R. (2016). miRNA-183-5p promotes cell proliferation and inhibits apoptosis in human breast cancer by targeting the PDCD4. *Reprod. Biol.* *16*, 225–233.
40. Li, C., Deng, L., Zhi, Q., Meng, Q., Qian, A., Sang, H., Li, X., and Xia, J. (2016). MicroRNA-183 functions as an oncogene by regulating PDCD4 in gastric cancer. *Anticancer. Agents Med. Chem.* *16*, 447–455.
41. Wei, C., Song, H., Sun, X., Li, D., Song, J., Hua, K., and Fang, L. (2015). miR-183 regulates biological behavior in papillary thyroid carcinoma by targeting the programmed cell death 4. *Oncol. Rep.* *34*, 211–220.
42. Lu, Y.Y., Zheng, J.Y., Liu, J., Huang, C.L., Zhang, W., and Zeng, Y. (2015). miR-183 induces cell proliferation, migration, and invasion by regulating PDCD4 expression in the SW1990 pancreatic cancer cell line. *Biomed. Pharmacother.* *70*, 151–157.
43. Yang, M., Liu, R., Li, X., Liao, J., Pu, Y., Pan, E., Yin, L., and Wang, Y. (2014). miRNA-183 suppresses apoptosis and promotes proliferation in esophageal cancer by targeting PDCD4. *Mol. Cells* *37*, 873–880.
44. Gu, W., Gao, T., Shen, J., Sun, Y., Zheng, X., Wang, J., Ma, J., Hu, X.Y., Li, J., and Hu, M.J. (2014). MicroRNA-183 inhibits apoptosis and promotes proliferation and invasion of gastric cancer cells by targeting PDCD4. *Int. J. Clin. Exp. Med.* *7*, 2519–2529.
45. Ren, L.H., Chen, W.X., Li, S., He, X.Y., Zhang, Z.M., Li, M., Cao, R.S., Hao, B., Zhang, H.J., Qiu, H.Q., and Shi, R.H. (2014). MicroRNA-183 promotes proliferation and invasion in oesophageal squamous cell carcinoma by targeting programmed cell death 4. *Br. J. Cancer* *111*, 2003–2013.
46. Li, J., Fu, H., Xu, C., Tie, Y., Xing, R., Zhu, J., Qin, Y., Sun, Z., and Zheng, X. (2010). miR-183 inhibits TGF- $\beta$ 1-induced apoptosis by downregulation of PDCD4 expression in human hepatocellular carcinoma cells. *BMC Cancer* *10*, 354.
47. Wang, H., Ma, Z., Liu, X., Zhang, C., Hu, Y., Ding, L., Qi, P., Wang, J., Lu, S., and Li, Y. (2019). miR-183-5p is required for non-small cell lung cancer progression by repressing PTEN. *Biomed. Pharmacother.* *111*, 1103–1111.
48. Sarver, A.L., Li, L., and Subramanian, S. (2010). MicroRNA miR-183 functions as an oncogene by targeting the transcription factor *EGR1* and promoting tumor cell migration. *Cancer Res.* *70*, 9570–9580.
49. Li, Z.B., Li, Z.Z., Li, L., Chu, H.T., and Jia, M. (2015). miR-21 and miR-183 can simultaneously target SOCS6 and modulate growth and invasion of hepatocellular carcinoma (HCC) cells. *Eur. Rev. Med. Pharmacol. Sci.* *19*, 3208–3217.
50. Salmena, L., Poliseno, L., Tay, Y., Kats, L., and Pandolfi, P.P. (2011). A ceRNA hypothesis: the Rosetta Stone of a hidden RNA language? *Cell* *146*, 353–358.
51. Li, M., Guan, H., Liu, Y., and Gan, X. (2019). lncRNA ZEB1-AS1 reduces liver cancer cell proliferation by targeting miR-365a-3p. *Exp. Ther. Med.* *17*, 3539–3547.
52. Hu, X., Li, Y., Kong, D., Hu, L., Liu, D., and Wu, J. (2019). Long noncoding RNA CASC9 promotes LIN7A expression via miR-758-3p to facilitate the malignancy of ovarian cancer. *J. Cell. Physiol.* *234*, 10800–10808.
53. Wu, L.L., Cai, W.P., Lei, X., Shi, K.Q., Lin, X.Y., and Shi, L. (2019). NRAL mediates cisplatin resistance in hepatocellular carcinoma via miR-340-5p/Nrf2 axis. *J. Cell Commun. Signal.* *13*, 99–112.
54. Wang, H., Huo, X., Yang, X.R., He, J., Cheng, L., Wang, N., Deng, X., Jin, H., Wang, N., Wang, C., et al. (2017). STAT3-mediated upregulation of lncRNA HOXD-AS1 as a ceRNA facilitates liver cancer metastasis by regulating SOX4. *Mol. Cancer* *16*, 136.
55. Li, S.P., Xu, H.X., Yu, Y., He, J.D., Wang, Z., Xu, Y.J., Wang, C.Y., Zhang, H.M., Zhang, R.X., Zhang, J.J., et al. (2016). lncRNA HULC enhances epithelial-mesenchymal transition to promote tumorigenesis and metastasis of hepatocellular carcinoma via the miR-200a-3p/ZEB1 signaling pathway. *Oncotarget* *7*, 42431–42446.
56. Fang, L., Du, W.W., Yang, X., Chen, K., Ghanekar, A., Levy, G., Yang, W., Yee, A.J., Lu, W.Y., Xuan, J.W., et al. (2013). Versican 3'-untranslated region (3'-UTR) functions as a ceRNA in inducing the development of hepatocellular carcinoma by regulating miRNA activity. *FASEB J.* *27*, 907–919.
57. Zhang, Q.H., Sun, H.M., Zheng, R.Z., Li, Y.C., Zhang, Q., Cheng, P., Tang, Z.H., and Huang, F. (2013). Meta-analysis of microRNA-183 family expression in human cancer studies comparing cancer tissues with noncancerous tissues. *Gene* *527*, 26–32.
58. Liang, Z., Gao, Y., Shi, W., Zhai, D., Li, S., Jing, L., Guo, H., Liu, T., Wang, Y., and Du, Z. (2013). Expression and significance of microRNA-183 in hepatocellular carcinoma. *ScientificWorldJournal* *2013*, 381874.
59. Ashmawy, A.M., Elgeshy, K.M., Abdel Salam, E.T., Ghareeb, M., Kobaisi, M.H., Amin, H.A.A., Sharawy, S.K., and Abdel Wahab, A.H.A. (2017). Crosstalk between liver-related microRNAs and Wnt/ $\beta$ -catenin pathway in hepatocellular carcinoma patients. *Arab J. Gastroenterol.* *18*, 144–150.
60. Bharali, D., Jebur, H.B., Baishya, D., Kumar, S., Sarma, M.P., Masroor, M., Akhter, J., Husain, S.A., and Kar, P. (2018). Expression analysis of serum microRNA-34a and microRNA-183 in hepatocellular carcinoma. *Asian Pac. J. Cancer Prev.* *19*, 2561–2568.
61. Zhang, X., Xu, P., Ni, W., Fan, H., Xu, J., Chen, Y., Huang, W., Lu, S., Liang, L., Liu, J., et al. (2016). Downregulated DYRK2 expression is associated with poor prognosis and oxaliplatin resistance in hepatocellular carcinoma. *Pathol. Res. Pract.* *212*, 162–170.
62. Hayashi, M., Nomoto, S., Kanda, M., Okamura, Y., Nishikawa, Y., Yamada, S., Fujii, T., Sugimoto, H., Takeda, S., and Kodera, Y. (2012). Identification of the A kinase anchor protein 12 (*AKAP12*) gene as a candidate tumor suppressor of hepatocellular carcinoma. *J. Surg. Oncol.* *105*, 381–386.
63. Xia, W., Ni, J., Zhuang, J., Qian, L., Wang, P., and Wang, J. (2016). miR-103 regulates hepatocellular carcinoma growth by targeting AKAP12. *Int. J. Biochem. Cell Biol.* *71*, 1–11.
64. Sun, J., Li, H., Huo, Q., Cui, M., Ge, C., Zhao, F., Tian, H., Chen, T., Yao, M., and Li, J. (2016). The transcription factor FOXN3 inhibits cell proliferation by downregulating E2F5 expression in hepatocellular carcinoma cells. *Oncotarget* *7*, 43534–43545.
65. Zhang, L., Li, S., Wang, R., Chen, C., Ma, W., and Cai, H. (2019). Anti-tumor effect of LATS2 on liver cancer death: role of DRP1-mediated mitochondrial division and the Wnt/ $\beta$ -catenin pathway. *Biomed. Pharmacother.* *114*, 108825.
66. Song, J., Zhao, W., Lu, C., and Shao, X. (2019). Retracted. *Cancer Cell Int.* *19*, 359.
67. Han, L.L., Yin, X.R., and Zhang, S.Q. (2018). miR-650 promotes the metastasis and epithelial-mesenchymal transition of hepatocellular carcinoma by directly inhibiting LATS2 expression. *Cell. Physiol. Biochem.* *51*, 1179–1192.
68. Han, L.L., Yin, X.R., and Zhang, S.Q. (2018). miR-103 promotes the metastasis and EMT of hepatocellular carcinoma by directly inhibiting LATS2. *Int. J. Oncol.* *53*, 2433–2444.
69. Bao, L., Yuan, L., Li, P., Bu, Q., Guo, A., Zhang, H., Cui, N., and Liu, B. (2018). A FUS-LATS1/2 axis inhibits hepatocellular carcinoma progression via activating Hippo pathway. *Cell. Physiol. Biochem.* *50*, 437–451.
70. Zhang, S., Wang, J., Wang, H., Fan, L., Fan, B., Zeng, B., Tao, J., Li, X., Che, L., Cigliano, A., et al. (2018). Hippo cascade controls lineage commitment of liver tumors in mice and humans. *Am. J. Pathol.* *188*, 995–1006.
71. Yi, J., Lu, L., Yanger, K., Wang, W., Sohn, B.H., Stanger, B.Z., Zhang, M., Martin, J.F., Ajani, J.A., Chen, J., et al. (2016). Large tumor suppressor homologs 1 and 2 regulate mouse liver progenitor cell proliferation and maturation through antagonism of the coactivators YAP and TAZ. *Hepatology* *64*, 1757–1772.
72. Lee, D.H., Park, J.O., Kim, T.S., Kim, S.K., Kim, T.H., Kim, M.C., Park, G.S., Kim, J.H., Kuninaka, S., Olson, E.N., et al. (2016). LATS-YAP/TAZ controls lineage specification by regulating TGF $\beta$  signaling and *Hnf4a* expression during liver development. *Nat. Commun.* *7*, 11961.
73. Guo, C., Wang, X., and Liang, L. (2015). LATS2-mediated YAP1 phosphorylation is involved in HCC tumorigenesis. *Int. J. Clin. Exp. Pathol.* *8*, 1690–1697.
74. Saito, Y., Li, L., Coyaude, E., Luna, A., Sander, C., Raught, B., Asara, J.M., Brown, M., and Muthuswamy, S.K. (2019). LGL2 rescues nutrient stress by promoting leucine uptake in ER<sup>+</sup> breast cancer. *Nature* *569*, 275–279.